View metadata, citation and similar papers at core.ac.uk
brought to you by CORE
provided by Hasanuddin University Repository

Proceedings of the 7th International Conference on Asian and Pacific Coasts (APAC 2013) Bali, Indonesia, September 24-26, 2013

THREE-DIMENSIONAL FLOW BEHAVIOR GENERATED BY SUSPENDED CANOPY

H. L. Tseung [1] and G. A. Kikkert [2]

ABSTRACT: Aquaculture, the farming of aquatic organisms, is a quickly growing industry responding to the worldwide increase in food demand. The physical interaction between the currents and aquaculture structures are important as these significantly influence the nutrients and waste fluxes in and surrounding aquaculture. Understanding the hydrodynamics is an important step to improve our overall knowledge of sustainable aquaculture practices. Geometrically, aquaculture structures can be modeled as suspended canopy, a porous media with very high porosity which is suspended downward from the free surface to some distance above the bottom boundary. Previous researchs on suspended canopy flow assume the flow is either one or two dimensional. However, the water flow in the field is three-dimensional and currents may be diverted underneath and around the canopy. The current paper presents results from experiments and numerical simulations to quantify the three-dimensional hydrodynamic effects of suspended canopy. Experiments were carried out by towing a canopy consisting of five times ten suspended elements through an existing towing tank. The towing velocity was constant at 0.10m/s. ADV was used to measure velocities at multiple locations surrounding the canopy. A finite element CFD model (Fluidity by AMCG) in combination with the k-ε or LES turbulence model were used to simulate the flow field generated by the moving canopy. Results were validated by using the ADV data. The presence of the canopy resulted in a reduction of the flow rate through the canopy of approximately 70%, measured at the trailing edge. Of the water diverted, 60% went around the canopy and 40% below the canopy.

Keywords: Aquaculture, suspended canopy, hydrodynamic, turbulence, acoustic doppler velocimetry, computational fluid dynamic

INTRODUCTION

Suspended canopies are porous media with high porosity and suspended downwardly from the free surface to some distance above the bottom boundary. Most aquaculture structures, especially shell fish farms, can be modeled as suspended canopy from a geometrical point of view (Plew, 2005; 2011). Note that, suspended canopy cannot be viewed as a reversed submerged canopy. Submerged canopy are a type of canopy which only occupy a part of the flow field from the bottom boundary to some distance below the water surface, and hence have an unbounded free-stream flow over it. In contrast, the flow below a suspended canopy is bounded by the bottom boundary.

The influence of suspended canopies on the local hydrodynamic characteristics have been observed and reported by researchers. For example, Strohmeier et al., (2005) have carried out field observations in southern Norway. They observed that a long-line mussel farm can reduce the water flow velocity coming into the farm and cause food depletion. Blanco et al. (1996) observed that raft-top connected mussel farms can both reduce the water flow velocity and affect the mixing processes within the farms.

Researchers point out that knowledge about the suspended canopy's influence on the water flow is important for producing efficient aquaculture management practices (Henderson et al., 2001), because these influences govern the fate and transport of input nutrients and aquaculture waste emissions (Chamberlain and Stucchi, 2007). Example research into the flow behavior generated by suspended canopy includes Plew (2005; 2011) who focused on the flow behavior generated by long line mussel farms. Delaux et al. (2010) carried out a two dimensional numerical simulation to study the interaction between water flow and long-line mussel farm. O'Donncha et al. (2013) employed two-dimensional physical and numerical models to assess the effects of aquaculture farm in Casheen Bary, Ireland.

One common point of these research studies is that they assume the flow within and around the suspended canopy is not three dimensional but either one or two dimensional. For example, in Plew's experiments, the flow parameters including the velocity only varied with

[1] Department of Civil and Environmental Engineering, Room 3573, Main Academic Building, The Hong Kong University of Science and Technology, Clear Water Bay, Kowloon, Hong Kong
[2] Department of Civil and Environmental Engineering, Room 3573, Main Academic Building, The Hong Kong University of Science and Technology, Clear Water Bay, Kowloon, Hong Kong

depth but were constant in both horizontal directions. The flow is also assumed fully turbulent, steady and uniform (Plew 2005; 2011). These assumptions are more convenient and numerically cheap once the study is focused on large scale problems (Plew, 2011). Furthermore, if the suspended canopy covers a significant area and the point of study is away from the edges, the non-three dimensional flow assumption should be reasonable. In that case the edge effects may be small enough that the error resulting from applying the non-three dimensional flow assumption throughout the canopy may be negligible. However, three dimensional hydrodynamic effects from a suspended canopy cannot be neglected when the study scale is smaller. In this case, the free-stream flow is modified by the interaction with the rows of suspended canopy elements when travelling past the canopy, but may not reach a steady-uniform state before reaching the end of the canopy and instead be a transitional flow throughout. In other words, the velocity will not only vary along the stream-wise direction but also the span-wise and vertical directions due to the modification as a result of the suspended canopy elements.

The purpose of this paper is to research the three-dimensional flow behavior generated by a suspended canopy. Due to the limited scope, the research in this paper focuses on the three dimensional flow field generated by a suspended canopy and the flow rate distribution once water passes through or around the canopy. The research has been divided into two parts. For the first part, a three-dimensional wooden and raft-top-connected suspended canopy was built. The physical model of the suspended canopy model was attached to a trolley and towed through water (in a water tank) at constant speed in the hydraulic laboratory located at the Hong Kong University of Science and Technology. Sontek 50 Mhz Acoustic Doppler Velocimeters (ADV) were used to measure the velocity at several locations surrounding the suspended canopy model. Analysis has been applied to the measured data to show the variation in the velocity when the water travelled past the canopy. For the second part, the suspended canopy model was rebuilt as a computer simulation and a 3-dimensional finite element CFD model, Fluidity, was used to simulate the flow field within and around the suspended canopy. Because turbulence plays an important role, both the k-ε and large eddy simulation methods were used. The CFD model was run with both simulation methods to enable a comparison of the simulated results with those of the experiments and determine whether either method is suitable for the prediction of the flow behaviour.

The paper is set up as follows: Section 2 describes the information related to the wooden suspended canopy model. Section 3 presents the acquisition of the velocity measurements with the ADV and the data analysis. Section 4 introduces the theory behind the Fluidity model and how it is set up for performing the numerical simulation. Section 5 shows the results and related discussion and Section 6 the conclusions.

SUSPENDED CANOPY MODEL

A wooden and raft-top-connected suspended canopy has been built and employed to reproduce the three dimensional flow behavior generated by real aquaculture suspended canopy (such as shellfish farms) in the laboratory. The raft top is 87 cm in length, 47cm in width and 2.5 cm in height. Fifty suspended elements were connected to the raft top, five per row and ten per column (Figure 1). The rows were parallel to the direction of the flow (which is in the stream-wise direction) and columns were perpendiculars to the direction of the flow. The spacing between each suspended element was 70mm in both the stream-wise and span-wise direction. Each suspended element was 25 mm in length, 25mm in width, and 300mm in height (Figure 2). Furthermore, the suspended canopy elements were all sufficiently rigid that they did not move due to the water current. The wooden suspended canopy model was placed inside a towing tank (length 16m, width 2m) at the center in the tangential direction. It was attached to a rigid aluminum framework which was part of a computer controlled trolley system that travelled length length-wise across the towing tank. The towing tank was filled with water to a height of 0.58m, so that the canopy elements were almost fully submerged in the water (Figure 2). The suspended canopy was towed through the tank at a constant speed of 10cm/s. For the remainder of the paper, the x-direction is defined as the stream-wise direction, the y-direction equals the span-wise direction, and the z-direction is the vertical direction. The origin is defined at the centre of the first row of elements as encountered by the water current (shown in Figure 1).

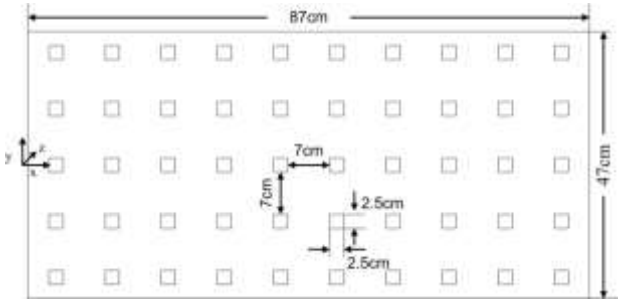

Fig 1. Plan view of the wooden suspended canopy model

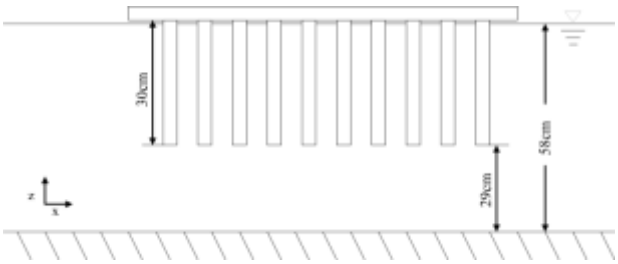

Fig 2. Side view of the wooden suspended canopy model once it was placed in the water tank

ACOUSTIC DOPPLER VELOCIMETER

Sontek 50 MHz side looking ADV has been used to measure the flow field near the suspended canopy while it was towed through the water tank. It measures the three dimensional velocity at a 2.5 mm^3 sample volume, 60 mm away from its transmitter and receivers based on the Acoustic Doppler principle (SonTek, 1997). The Acoustic Doppler principle means that the ratio of the velocity at the sample volume to the velocity scattered back to the ADV receiver from the sample volume is proportional to the acoustic frequency that is emitted by the ADV to the frequency received by the ADV. It has been proven that the ADV has a good capability to measure turbulent velocity, such as in estuary (Chanson et al, 2008). Furthermore, the operation and the set up of the ADV are relatively easy when compared to other velocimeters. Therefore ADV is adopted for this research.

The ADV was used to measure the flow velocity at 26 points surrounding the suspended canopy model. Along the centerline of the canopy in the y-direction, velocities were obtained at 5 points at the front and 5 points at the back of the canopy. In addition, measurements were obtained at 8 points along each of the two sides of the canopy. The 8 points along the sides were located 10cm away from the canopy and all ADV measurement points were located 10cm below the canopy model. The ADV was held in position by a rigid arm that was attached directly to the canopy. Seeding particles were added to the water to increase the back scatter capacity of the water to reduce the error of the ADV velocity measurement (Sontek, 1997). At each measurement point, the velocity data was measured twice. One was recorded when the trolley moved forwards (along the x-direction), the other one was recorded when the trolley moved backwards.

After obtaining the measurements, processing of the raw data was carried out. Firstly, the data at the start of the recording before the flow reached steady state and the data at the end of the recording when the trolley velocity was no longer 10 cm/s was removed. Secondly, velocity data at a particular time step that was different from the data at the previous and next time step by more than 3 cm/s was identified as erroneous, removed and replaced with a mean value of the previous and next time step. The limit of 3cm/s removed the extreme spikes without removing the fluctuations due to turbulence. Thirdly, the forward and backward measurements were all transformed into the coordinate system mentioned above. The time-series from forward and backward measurements that were recorded at the same location were then combined.

Once the processing was completed, Reynolds decomposition formula was used to decompose the data into a mean flow and fluctuating component:

$$u_{(x,v,z,t)} = \overline{u_{(x,v,z,t)}} + u'_{(x,y,z,t)} \quad (1)$$

where u is the instantaneous velocity, $\bar{u}$ is the time averaged velocity and u' is the fluctuating part. The mean flow is used in the comparison with the results from the Fluidity simulation. The error in the fluctuating velocity data was too great to be used for the comparison with the numerical data because the time-series recorded was not long enough.

Although the ADV is a convenient tool for measuring the flow velocities around the suspended canopy model, it has two major limitations. Firstly, it is an intrusive velocimeter, hence it is impossible to use it to measure the flow field within the suspended canopy model. Secondly, ADV is a point velocimeter. It is cumbersome to use ADV to measure the whole field. CFD is adopted to cover the limitations of ADV.

FLUIDITY MODEL

Fluidity, an open source, multi-purpose, CFD code has been used to simulate the flow field within and around the suspended canopy model (AMCG, 2012). It is developed by the Applied Modeling and Computation Group. This group belongs to the Department of Earth Science and Engineering at the Imperial College London. Fluidity adopts the finite element method (FEM) to approximate the Navier-Stokes equation. FEM does not solve the Navier-Stokes equation directly; instead it solves the weak formulation of this equation. The weak formulation is a weighted-integral residual statement that is equivalent to both the differential equation as well as the associated boundary conditions (Reddy and Gartling, 2001). Fluidity uses the Galerkin method, a weighted residual method, to develop the weak formulation of the Navier-Stokes equation (AMCG, 2012). Galerkin's method is based on a set of linearly independent test

functions to represent the weight for minimizing the residual (Chung, 1978). In Fluidity, polynomial functions which are derived according to the geometry of the mesh cell are used for the test function (AMCG, 2012).

The weak formulation that Fluidity uses to find the approximated solution of the Navier-Stokes equation is written as follow:

$$M\frac{du}{dt} + A(u)\bullet u + K\bullet u + C\bullet p = 0 \qquad (2)$$

where u is the velocity vector, t is the time, and p is the pressure. Within equation (2), M is the mass matrix which is defined as

$$M = \int_{\Omega} \rho \Phi_i \Phi_j \qquad (3)$$

In the definition of the mass matrix, Ω is the computation domain, ρ is the fluid density, Φ is the test function and i and j are the matrix index. A in equation (2) is the advection matrix:

$$A = \int_{\Omega} \Phi_i (\rho u \nabla \Phi_i) \qquad (4)$$

K is the viscosity matrix and it is written as:

$$K_{ij} = \sum_{(\alpha,\beta,\gamma)} \int_{\Omega} (\partial_\beta \Phi_{i,\alpha}) \overline{\overline{k_{\beta,\gamma}}} (\partial_\gamma \Phi_{i,\alpha}) \qquad (5)$$

where α, β, and γ are indexes for the summation over spatial domain. $\overline{\overline{k_{\beta,\gamma}}}$ is the diffusion coefficient tensor. Finally C is the pressure gradient matrix and it is defined as

$$C_{ij} = \int_{\Omega} \Phi_i \nabla \Phi_j \qquad (6)$$

For this paper, an unstructured mesh with 15033 nodes and 84117 elements has been built to describe the suspended canopy model and the water with an external mesh creating software Gmsh as suggested by AMCG. Figure 3 shows the mesh used for the numerical experiment. The numerical suspended canopy model is fixed at the center of the numerical water tank and water is set to flow into the tank constantly with a speed of 10 cm/s from the inflow boundary. The total running period of both the k-epsilon and LES model is 240 seconds to make sure the flow has reached steady state. Both k-epsilon and LES (Smagorinsky second order model) models have been adopted to simulate the flow through and surrounding the suspended canopy. The time averaged mean velocities are compared with the ADV measurements to evaluate the accuracy of the model predictions, before the model results are used to investigate the 3D hydrodynamic characteristics of the flow around the suspended canopy model in more detail.

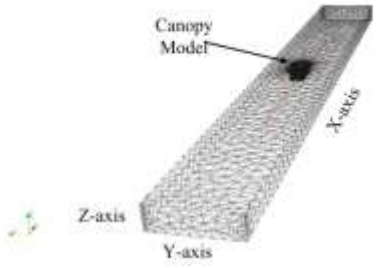

Fig 3. Computational mesh for numerical simulation study on the effects generated by the suspended canopy model

RESULTS AND DISCUSSIONS.

Comparisons between the measured mean velocity data at the 26 measurement points and the corresponding time averaged Fluidity simulated mean velocities are show in Figure 4 to Figure 6. Note the results presented were obtained at a vertical depth 10 cm below the canopy elements. In general, there is reasonably good agreement between the measurements and the simulated results with each of them showing the same trends. However, in terms of the magnitude of the velocities, some differences can be observed and these are mainly between the experiments and the simulations and less between the two simulations themselves.

Figure 4a presents the results at the location along the centerline and in front of the canopy. The mean velocity in the x-direction, u, is lower than that of the free-stream for all measurement locations, i.e. water more than 30 cm away from the front of the canopy is already aware of its presence. Closer to the canopy, the water velocity drops further, however a significant increase occurs at approximately 8 cm before the canopy. Additional information from the simulation indicates that this is related to the acceleration of water that is being diverged below the canopy. Even closer to the canopy, the velocity has reduced again as it begins to be affected by the shear layer generated below the canopy (Plew et al., 2006). The magnitude of the variations in the velocity in the 10 cm closest to the canopy are greater for the measured data, but the model results are in good agreement. The velocity in the y-direction, v, is presented in Figure 4b. Because of symmetry in the canopy and the set up in the towing tank, the velocity is expected to be close to zero. The results confirm this to a certain extent, although there are small variations present. These variations are again bigger for the measured

results. The vertical velocity, *w* and shown in Figure 4c, is downwards at all measurement locations and within the 10cm closest to the canopy, the flow accelerates due to divergence of water below the canopy.

Along the centerline at the back of the canopy, the velocity in the x-direction (Figure 5a) is lower than at the front of the canopy, and it is increasing only very gradually with distance downstream. At the end of the simulated domain, the velocity only increased back to 80% of the free-stream velocity in both k-ε and LES simulations. The variation in the measured velocity is approximately equal to the differences in the estimates from the simulations. The velocity in the y- direction is still approximately zero (Figure 5b) and the and the velocity in the z-direction (Figure 5c) is positive, and therefore upwards, close behind the canopy as the water flow readjusts after being diverted because of the canopy. The negative velocities obtained by the ADV at the final two measurement locations are an indication of the existence of a trapped vortex behind the canopy. The simulated results also predict this vortex, but the distance behind the canopy is slightly greater. The simulated results show that the end of the trapped vortex is at approximately 1.5 m behind last row of the suspended canopy elements (again the k-ε and LES both gave similar results). Further downstream, oscillations between small upwards and downwards velocities are predicted. These oscillations are stronger in the k-epsilon simulation, and persist throughout the simulated domain.

The velocity results at the side of the canopy are presented in Figure 6. At the measurement location closest to the front of the canopy, the velocity in the x-direction (Figure 6a) is higher than the free-stream velocity. In addition to water being accelerated below the canopy, water also accelerates around the canopy.

a)

b)

c)

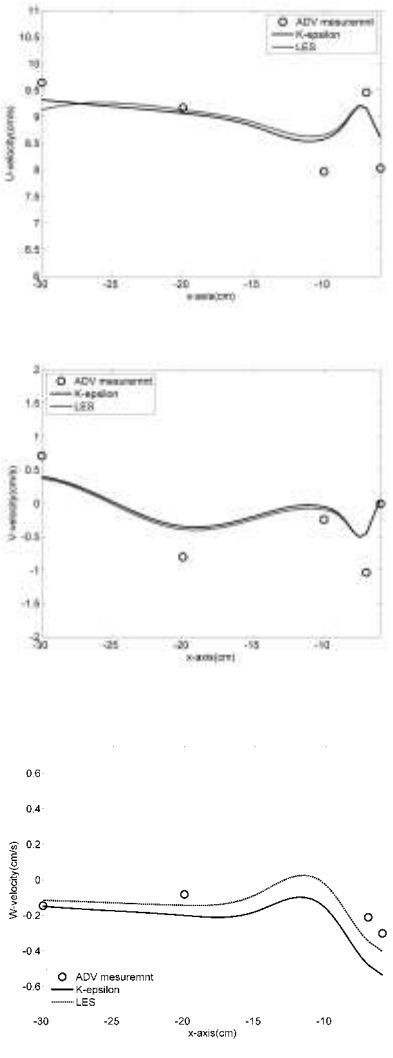

Fig 4. Comparison between the ADV measured and Fluidity simulated *u* velocity (a), *v* velocity (b) and *w* velocity (c) at the front of the suspended canopy

a)

b)

c)

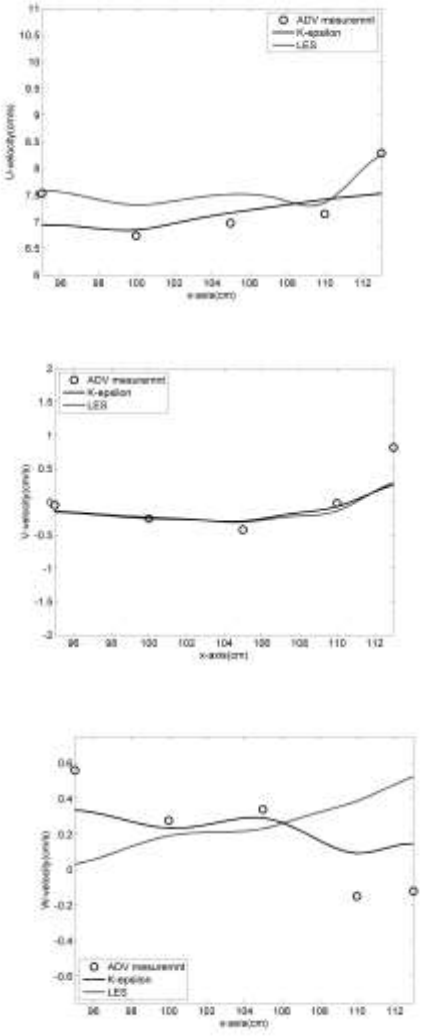

Fig 5. Comparison between the ADV measured and Fluidity simulated *u* velocity (a), *v* velocity (b) and *w* velocity (c) at the back of the suspended canopy

a)

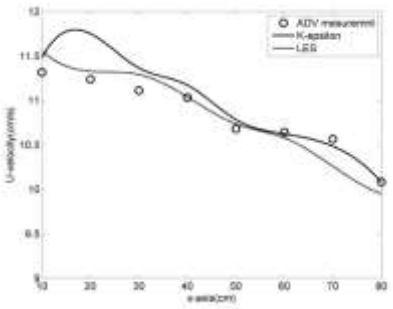

b)

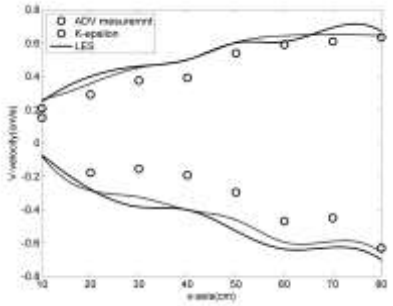

c)

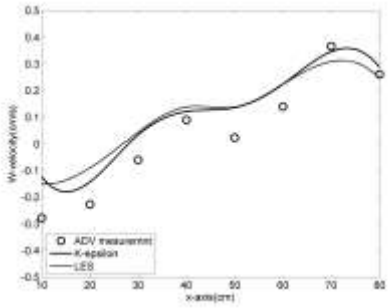

Fig 6. Comparison between the ADV measured and Fluidity simulated *u* velocity (a), *v* velocity (b) and *w* velocity (c) at the side of the suspended canopy

However, the velocity does not remain constant alongside the canopy, instead it decreases with distance away from the front. Additional information from the simulation showed that a shear layer of increasing thickness develops alongside the canopy. In addition, increasing volumes of fluid that enter the canopy at the front exit the canopy at the sides, as indicated by the increasing positive velocity in the y-direction on the starboard side and increasing negative velocity on the port side of the canopy (Figure 6b). The velocity in the z-direction is initially negative and thus downwards, as water is diverted below the canopy, but changes approximately half-way along the canopy to become positive and thus upwards. Additional information from the simulations showed that at 10 cm below the actual canopy, the vertical velocity remained negative along the whole length of the canopy, but is still smaller near the back than near the front of the canopy. This indicates that during the initial diversion of water near the front, it overshoots its equilibrium depth which may be related to the proximity of the bottom boundary. Further down the canopy the water flow readjust causing smaller negative velocity below the canopy as water still exits the canopy through the bottom boundary. As this is not present at the sides of the canopy, the readjustment of the water flow causes the vertical velocities to become positive. The velocity results along the starboard and port sides of the canopy showed similar trends, however some differences were also observed which indicates flow asymmetry surrounding the canopy in both the experimental as well as the simulated results. For example the x-velocities on the starboard and z-velocity on the port side were slightly greater. The precise reason for this asymmetry requires additional research. In neither direction does the velocity become constant alongside the canopy, indicating that indeed the flow surrounding the canopy was transitional throughout.

The velocity data has confirmed that the water is diverted below and around the canopy, however it has also indicated that the water that does enter the canopy at the front may not simply leave the canopy at the back, but instead leave the canopy through either the sides or the bottom. A shear layer develops at either side and at the bottom of the canopy, however the simulated results showed that this also occurs inside the canopy at either side of a column of elements. The development of these internal shear layers means that the average velocity in the x-direction of water inside the canopy decreases with increasing distance in the canopy and the flow is increasingly diverted either in the y or z-directions. To quantify the diversion of water flow surrounding the canopy, and therefore estimate the blocking effects by the canopy elements toward the mass transport, a flow rate analysis has been carried out. Only the simulated velocity results are used for this analysis. Within the computational domain of the simulation 21 cross sections perpendicular to the direction of the free-stream flow are selected. All cross sections are divided into 4 zones (Figure 7), the water flux through zones 1 (starboard) and 2 (port) represent the flow rate at either side of the canopy, the water flux through zone 3 represents the flow rate through the canopy and the water flux through zone 4 represents the flow rate below the canopy. The areas of zone 1 and zone 2 are 0.291 m^2, the area of zone 3 is 0.194 m^2 and the area of zone 4 is 0.387m^2. The flow rate for each zone at each cross-section is computed by using the Q=UA, where U is the average velocity of the flow in the x-direction passing through the zone. The computed flow rates then are used

to estimate the flow rate modification ratio (QMR) for each zone. The formula is listed as follows:

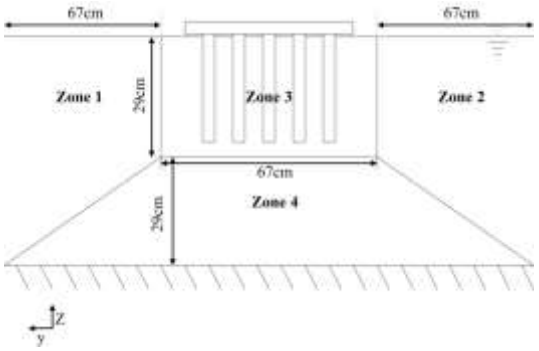

Fig. 7. Zone separation for estimated flow rate depletion analysis.

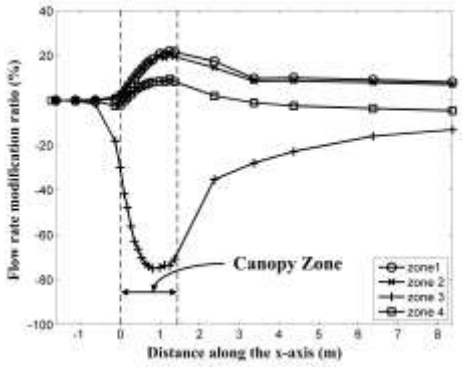

Fig. 8. Flow rate modification ratio for the four selected zones along the x-axis based on the k-epsilon simulation results. The location of the suspended canopy model is marked in the figure.

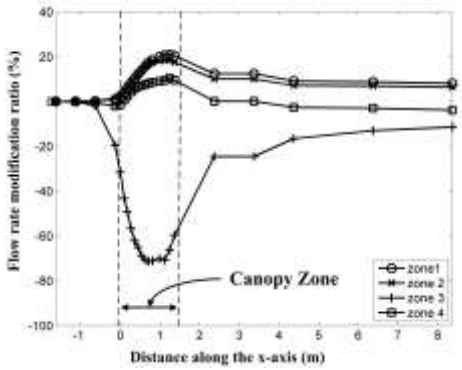

Fig. 9. Flow rate modification ratio for the four selected zones along the x-axis based on the LES simulation results. The location of the suspended canopy model is marked in the figure.

$$QMR = \left[\left(Q_i - Q_1 \right) / Q_1 \right] \cdot 100\% \quad , i = 1, 2, 3, ..., 21 \qquad (7)$$

where *i* is the index for the cross section. The first cross-section is located 1.63 m in front of the canopy and the flow rate in all zones is therefore not affected by the canopy and can therefore be used to assess the modification of the flow rate due to the presence of the canopy. Figure 8 and 9 show the flow rate modification ratios calculated using the k-ε and LES simulated results respectively. In these figures, the markers represent the computed QMR at each of the cross-sections and the curve is the trend line. The results from the two simulations are again very similar. The flow rate at the side of the canopy starts to increase from 0.13 m in front of the canopy onwards. Initially this increase is relatively slow, but at x = 0.18 m the increase become much more rapid. The maximum coincides approximately with the end of the canopy and both simulations give an estimate for the increase in flow rate of more than 20%. In the first 2 meters behind the canopy, the flow rate decrease relatively quickly, while for the remainder of the flow domain the decrease is very gradual, which is related to the very gradual change in the x-velocity behind the canopy mentioned previously. Again some asymmetry can be observed in the results, the flow rate through the starboard zone is higher because of the higher velocity in the x-direction mentioned earlier. The modification of the flow rate below the canopy is similar to that at the side, although there is no increase observed in front of the canopy, instead there is a small decrease initially, and the maximum flow rate is reached just before the end of the canopy where the flow rate has increased by approximately 10%. In absolute terms this means that of the water diverged, 60% was diverged around the canopy and 40% below the canopy. The influence of the proximities of the side walls and the bottom of tank on these values requires more research.

The flow rate through the canopy, zone 3, reduced very quickly once inside the canopy, which is in agreement with field observation by Strohmeir et al. (2005). The reduction increases from 20% at the front of the canopy to more than 70% at the end of the canopy. The 70% reduction in flow rate corresponds to a reduction of the average velocity between the canopy elements of 63%, which corresponds well with measurements in the field in various aquaculture structures by Gibbs et al. (1991) of 70%, Grant and Bacher (2001) of 54% and Plew (2005) of 47% to 67%.

SUMMARY AND CONCLUSION

The hydrodynamics of a flow surrounding a wooden raft-top-connected suspended canopy has been studied through ADV measurements and Fluidity model simulations. The length and width of the suspended canopy were limited so that the canopy generated a three-dimensional flow field.

The comparison of the ADV mean velocity results and the simulated velocity results showed that in general the model predictions are in agreement with the experimental data and that the difference between the results of the k-epsilon and LES simulations is small. Furthermore, the velocity results showed that the flow throughout the canopy was transitional, water accelerated around and below the canopy as a result of the obstacle present in its path and some of the water that entered the canopy at the front exited the canopy either through the sides or through the bottom of the canopy. The flow rate inside the canopy reduced by more than 70%, corresponding with an average velocity decrease of 63% and of the water diverted, 60% went around the canopy and 40% below the canopy.

In the current study, only a single suspended canopy has been used, therefore the effects of the canopy density, canopy shape and proximities of bottom and side wall boundaries on the three-dimensional flow rate are still unknown. Preparations are underway to carry out experiments whereby each of the variables can be changed and its effects of the flow field be measured.

Finally. the limitations of the ADV, point measurements only and no measurements inside the canopy, make it an unsuitable measurement instrument for obtaining experimental data that allows a more detailed assessment of the prediction capabilities of the simulations. Hence further tests will be carried out using PIV instead, which would also allow the vortex structures and the associated mixing to be studied.

REFERENCES

AMCG, (2012) Fluidity manual (version 4.1 branch), Department of Earth Science and Engineering, Imperial College London < http://amcg.ese.ic.ac.uk/index.php?title=Fluidity>

Blanco, J., Zapata, M., and Morono., A. (1996) Some aspects of the water flow through mussel rafts, Sci. Mar., 60(2-3): 275-282

Chamberlain J., and Stucchi D. (2007) Simulating the effects of parameter uncertainty on waste model predictions of marine finish aquaculture, Aquaculture, 272:296-311

Chanson, H., Trevethan, M., and Aoki S., (2008) Acoustic Doppler velocimetry (ADV) in small estuary: Field experiment and signal post-processing, Flow Meas. Instrum., 19:307-313

Chung, T.J (1978) Finite element analysis in fluid dynamics, McGraw-Hill: New York, USA

Delaux, S., Stevens, C.L., and Popient S., (2010) High resolution computational fluid dynamic modeling of suspended shellfish structure, Environ. Fluid Mech., 11(4):405-425

Gibbs, M.M., James, M.R., Pickmere S.E., Woods P.H., Shakespeare B.S., Hickman R.W. and Illingworth J., (1991). Hydrodynamic and water column properties at six stations associated with mussel farming in Pelorus Sound, 1984-85. New Zeal. J. Mar. Fresh. 25: 239-254.

Ghisalberti, M., (2009) Obstructed shear flows: similarities across systems and scales, J. Fluid Mech., 641: 51-61

Ghisalberti, M., (2010) The three-dimensionality of obstructed shear flows, Environ. Fluid Mech., 10:329-343

Ghisablerti, M., and Nepf H., (2005) Mass transport in vegetated shear flows, Environ. Fluid Mech., 5:527-551

Grant, J. and Bacher C., (2001). A numerical model of flow modification induced by suspended aquaculture in a Chinese Bay. Canadian J. of Fisheries and Aquatic Sciences, 58: 1003-1011.

Henderson, A., Gamito, S., Karakassis, I., Pederson, P., and Smaal A., (2001) Use of hydrodynamic and benthic models for managing environmental impacts of marine aquaculture. Appl. Ichthyol.17:163-172

Park ,C.W. and Lee, S.J., (2000) Free end effects on the near wake flow structure behind a finite circular cylinder, J. Wind Eng. Ind. Aerodyn,88:231-246

O'Donncha, F., Hartnett, M., and Nash, S. (2013) Physical and numerical investigation of the hydrodynamic implication of aquaculture farms, Aquac. Eng, A.E.S., 52:14-16

Plew, D.R. (2005), The hydrodynamic effect of long-line mussel farm, PhD dissertation, University of Canterbury (New Zealand)

Plew, D.R., Spigel, R.H., Stevens, C.L., Nokes, R.I., and Davidson, M.J.,(2006) Stratified flow interactions with a suspended canopy, Environ. Fluid Mech., 6:519-539

Plew, D.R. (2011), Depth-averaged drag coefficient for modeling flow through suspended canopies, J. Hydraul. Eng., ASCE, 137(2): 234-247

Reddy J.N., and Gartlin D.K., (2001) The finite element method in heat transfer and fluid dynamics (2nd edition), CRC press: Boca Raton, USA

Sontek (1997) Sontek Acoustic Doppler Velocimeter Technical Document, San Diego, CA

Strohmeier T., Aure J., Duinker A., Castberg T., Svardal A. and Strand O., (2005) Flow reduction, seston depletion, meat content and distribution of diarrhetic shellfish toxins in a long-line blue mussel (Mytilus Edulis) farm, J. Shell Res., 24 (1):15-23